Cluster radioactivity of actinide nuclei by the emission of Ne, Mg, and Si isotopes: A semiempirical analysis of the half-lives*

O. A. P. Tavares and E. L. Medeiros[1]

Centro Brasileiro de Pesquisas Físicas - CBPF/MCTI
Rua Dr. Xavier Sigaud 150, 22290-180 Rio de Janeiro-RJ, Brazil

In celebration of the centenary of the birth of Prof. César Lattes, one of the discoverers of π-meson and founders of CBPF (Rio de Janeiro).

Abstract - Partial half-lives of exotic radioactive decays of Th, Pa, U, Pu, and Cm parent isotopes by the emission of Ne, Mg, and Si isotopes is re-evaluated in the framework of a semiempirical, one-parameter model based on the quantum tunneling mechanism through a potential barrier where the Coulomb, centrifugal and overlapping contributions to the barrier are considered within the spherical nucleus approximation. Updated values of nuclear mass and radius of the participating nuclides caused measured half-life data to be reproduced with better reliability. The calculation model can be applied to other heavy-cluster decay cases of heavy and superheavy nuclei. It is found a quite linear correlation of decimal log of half-life with the area between the potential barrier curve and the Q-value for decay along the total barrier region.

Keywords: cluster radioactivity, actinide nuclei, Ne isotopes, Mg isotopes, Si isotopes, semiempirical model, half-life systematics.
PACS: 23.70.+j, 27.90,+b

[1] Corresponding author. E-mail: emildelimamedeiros@gmail.com

1 Introduction

The radioactive disintegration process by the emission of nuclear fragments heavier than the alpha particle, named today cluster radioactivity or exotic decay, was originally known as spontaneous emission of heavy-ions (or clusters) from heavy nuclei [1–4], and subsequently used in Refs. [5–7].

The possible existence of such a rare spontaneous disintegration process was considered quantitatively for the first time early in 1975–1976 by de Carvalho *et al.* [1, 2]. At that time, despite inaccuracies in both nuclear mass- and radius-values, very preliminary calculations based on the semi-classical mechanism of penetration through a potential barrier, like the quantum tunneling model of alpha-particle decay process, had indicated the possibility of a few heavy fragments being emitted from ^{238}U parent nucleus. Those early calculations showed that shell effects were clearly manifested since results had indicated magic numbers of nucleons in the product nuclides of most likely emission modes [2–4]. Such studies had been motivated by the observation of strange, short-range tracks (as compared with ordinary fission fragment tracks) recorded in nuclear-track emulsion loaded with uranium aimed at re-measuring of its spontaneous fission rate [2].

These surprising, novel results were interpreted soon afterwards by Sandulescu, Greiner and Poenaru [8–10] as a case of very large asymmetry in the break-up of heavy fissile nuclei carried by shell effects of one or both fragments (a historical account on this subject is reported in [11–13]).

In the middle of 1980s theoretical investigations on exotic decays [5–7] stimulated a number of experimental research groups to identify and measure the activity of rare, possible cases of decay by cluster emission of extremely small ($\sim 10^{-16}$–10^{-9}) predicted branching ratios relative to alpha decay. So it was that the first experimental identification of a case of decay by the emission of nuclear fragments heavier than the alpha particle was accomplished by Rose and Jones [14] from the University of Oxford (UK), who reported the observation of $^{223}\mathrm{Ra} \rightarrow {}^{14}\mathrm{C}$ decay with a half-life of $(3.7 \pm 1.1) \times 10^7$ a. This finding was confirmed soon afterwards and independently by four groups of experimentalists [15–18] obtaining a weighted average half-life of $(4.8 \pm 0.5) \times 10^7$ a, followed by the observation of a fine structure in such a decay process [19–20].

Subsequently, a number of new cases of cluster radioactivity of heavy nuclei from ^{221}Fr up to ^{242}Cm was observed involving the emission of fragments heavier than ^{14}C, such as ^{20}O, ^{22,24,26}Ne, $^{28-30}$Mg, and ^{32,34}Si isotopes. At the moment, almost thirty cases of exotic decays have been experimentally identified, and their partial half-lives measured in the region of translead parent nuclei [21–23]. This phenomenon is indeed a very rare nuclear process since the observed branching ratios relative to alpha decay vary from 1.4×10^{-16} ($^{238}\mathrm{Pu} \rightarrow {}^{32}\mathrm{Si}$ [24]) to 0.85×10^{-9} ($^{223}\mathrm{Ra} \rightarrow {}^{14}\mathrm{C}$ [14]). The reader is referred, for instance, to publications by Zamyatnin *et al.* [25], Gonçalves and Duarte [26], Poenaru [27], Tretyakova *et al.* [28], Kuklin *et al.* [29], Hourani *et al.* [30], Poenaru and Greiner [31], and references quoted therein in all these papers which give detailed description of this phenomenon from both the experimental and theoretical points of view.

It is worthwhile to mention the golden rule of exotic decays announced by Ronen [32] who stated

that the most favorable parent nuclei for cluster emission are those that emit clusters which have the highest binding energy per total number of blocks of deuterons and tritons (^{14}C, ^{24}Ne, ^{28}Mg, ^{34}Si) and the daughter nuclei are preferred magic (or semi-magic) close to the double magic ^{208}Pb isotope.

The physical analogy between alpha decay and cluster radioactivity has given rise to phenomenological studies to unify these two nuclear decay processes looking for general formulas to reproduce the measured half-lives. Such investigations have been reported, for instance, in [33, 34]. In addition, as pointed out by Poenaru *et al.* [35], the radioactive cluster decay process was extended to superheavy parent nuclei ($Z > 110$), showing predominance of some cluster decay cases over the well-known alpha decay when the daughter nuclei were located around ^{208}Pb isotope, allowing emitted clusters of $Z > 28$. This pioneering study of cluster decay in the region of superheavy nuclei was followed with similar calculations by Zhang and Wang [36] and Warda *et al.* [37].

Motivated by the surprising discovery of a rare alpha-particle activity in the naturally occurring ^{209}Bi isotope (100% isotopic abundance), with a measured half-live of $(1.9 \pm 0.2) \times 10^{19}$ a [38], we developed for the first time a one-parameter, semiempirical calculation model based on the quantum mechanical tunneling mechanism through a potential barrier, like the one introduced early in 1928 by Gamow [39] and Gurney and Condon [40], to reproduce such a measurement. The model was constructed following the lines of the current alpha decay theory of penetration through a Coulomb plus centrifugal potential barriers, additionally including the overlapping of the nascent fragments via a semiempirical potential barrier [41]. Such a model will be named henceforth alpha decay like model (ADLM). When it was applied to alpha decay of bismuth isotopes a half-life of $(1.0 \pm 0.3) \times 10^{19}$ a was predicted for ^{209}Bi isotope [41], a value very close to the one found from the experiment [38].

The ADLM was successfully applied to platinum isotopes [42], to a systematic study of a large number (~ 330) of alpha-emitter nuclides [43], and also extended to known cases of radioactivity by the emission of one-proton [44] and heavy clusters (C, N, O, F, Ne, Mg, and Si isotopes) from translead parent nuclei as well [12, 13]. More recently, the ADLM has been used to systematize alpha decay half-life data of osmium isotopes [45] and hafnium isotopes [46], to obtain an accurate half-life value of ^{147}Sm [47] and ^{146}Sm [48] isotopes, and of the long-lived ($T_{1/2} = 31$ a) ^{178}Hf^{m2} isomer [49]. ADLM predictions for partial half-lives of two-proton radioactive decay process have been also successfully obtained for known cases of $A < 68$ nuclides located in the vicinity of proton drip line [50].

By considering the current, updated data of nuclear masses [51], half-lives [52], as well as nuclear radii [53] we thought it would be worth reviewing the ADLM applied to exotic decay cases. In this context, in the present work we chose to undertake a systematic analysis of the half-lives of exotic decays of ^{230}Th, ^{231}Pa, $^{230,232-236}$U, ^{236,238}Pu, and ^{242}Cm parent nuclei by the emission of ^{22,24,26}Ne, $^{28-30}$Mg, and ^{32,34}Si isotopes by applying our semiempirical, one-parameter ADLM in its updated version. This calculation model can be used in obtaining half-life predictions for other already known cases of exotic decays or not yet experimentally observed ones, as well as extended to those cluster decays in the region of superheavy parent nuclei.

2 ADLM to evaluate partial half-lives of radioactive cluster decays

Just over a decade ago we have reported in details a version of our ADLM, which is based on the current quantum tunneling mechanism through an overlapping-plus-Coulomb-plus-centrifugal potential barrier within the spherical nucleus approximation [13]. In the overlapping region (Fig. 1), following previous descriptions by Duarte and Gonçalves [54] and Poenaru *et al.* [6], we have assumed for both quantities the reduced mass, $\mu(s)$, and potential barrier, $V(s)$, of the disintegrating system (s is separation between the centers of the nascent fragments), respectively, power functions of $s-a$ ($a \leq s \leq c$), *viz.*

$$\mu(s) = \mu_0 \left(\frac{s-a}{c-a}\right)^p, \; p \geq 0 \tag{1}$$

$$V(s) = Q + (V_c - Q)\left(\frac{s-a}{c-a}\right)^q, \; q \geq 1 \tag{2}$$

where the total potential energy at contact configuration, V_c, is calculated as

$$V_c = \frac{Z_{\mathsf{C}} Z_{\mathsf{D}}\, e^2}{c} + \frac{\ell(\ell+1)\,\hbar^2}{2\mu_0 c^2}\,. \tag{3}$$

Here, $e^2 = 1.43996444$ MeV·fm is the square of the electronic elementary charge, ℓ is the mutual orbital angular momentum resulting from the rotation of the disintegration product nuclei around their common center of mass, $\hbar = h/(2\pi) = 6.582119 \times 10^{-22}$ MeV·s is Planck's constant, μ_0 is the effective reduced mass of the already formed fragments in the separation region ($c \leq s \leq b$, Fig. 1), $a = R_{\mathsf{P}} - R_{\mathsf{C}}$ is the difference between the radius of the parent nucleus and the cluster radius, $c = R_{\mathsf{D}} + R_{\mathsf{C}}$ is the position of the configuration at contact of the preformed fragments (R_{D} denotes the radius of the daughter nucleus), Q is the total disintegration energy, *i.e.* the Q-value of the decay process, and the Z's are the atomic numbers of the product fragments.

Denoting by G the semiclassical WKB-integral approximation, *i.e.* Gamows factor for decay, we have for the overlapping region

$$G_{\mathsf{ov}} = \frac{1}{\hbar}\int_a^c \sqrt{8\mu(s)[V(s)-Q]}\,\mathrm{d}s\,. \tag{4}$$

The quantity $S = \exp(-G_{\mathsf{ov}})$ represents, therefore, the preformation probability, or the "arrival" of the cluster to the nuclear surface. S sometimes is known as the spectroscopic factor, which is strongly related to the complexity of the cluster to be formed. By inserting (1)–(3) into (4), and for convenience defining the dimensionless quantities

$$x = \frac{\ell(\ell+1)\hbar^2}{2\mu_0 c^2 Q} \quad \text{and} \quad y = \frac{1}{2}\frac{Z_{\mathsf{C}} Z_{\mathsf{D}}\, e^2}{c\,Q}\,, \tag{5}$$

it results

$$G_{\mathsf{ov}} = \frac{1}{\hbar}\sqrt{8\mu_0 Q}\,(c-a)\cdot H(x,y)\cdot g_{\mathsf{se}}\,, \tag{6}$$

with

$$H(x,y) = \sqrt{x + 2y - 1}\,. \tag{7}$$

In the expression (6) for G_{ov} the quantity

$$g_{\mathsf{se}} = \frac{1}{(p+q)/2 + 1} \tag{8}$$

is the semiempirical, one-parameter of the present model, the value of which is thus determined from a set of half-life measurements. In calculating G_{ov}, the parameter g_{se} results as a combination of the unknown exponents p and q which appear in (1) and (2).

In the separation barrier region created by the just formed fragments ($c \leq s \leq b$, Fig. 1) the total potential energy is the sum of Coulomb plus centrifugal contributions, $V_{\mathsf{t}}(s) = V_{\mathsf{Coul}} + V_{\mathsf{cent}}$ and, therefore, Gamows factor for this tunneling region is calculated as

$$G_{\mathsf{sp}} = \frac{1}{\hbar}\sqrt{8\mu_0 Q}\int_c^b \sqrt{2y\left(\frac{c}{s}\right) + x\left(\frac{c}{s}\right)^2 - 1}\,\mathrm{d}s\,, \tag{9}$$

where b is the solution of $V_{\mathsf{t}}(b) = Q$. The quantity $P = \exp(-G_{\mathsf{sp}})$ represents the penetrability factor through the external, separation barrier region. The calculation of (9) gives the expression for G_{sp} as

$$G_{\mathsf{sp}} = \frac{\sqrt{8}\,e^2}{\hbar}\,Z_{\mathsf{C}}Z_{\mathsf{D}}\sqrt{\frac{\mu_0}{Q}}\cdot F(x,y)\,, \tag{10}$$

where

$$F(x,y) = \frac{\sqrt{x}}{2y}\cdot\ln\left(\frac{\sqrt{x}\cdot H(x,y) + x + y}{\sqrt{x+y^2}}\right) + \arccos\sqrt{\frac{1}{2}\left(1 - \frac{y-1}{\sqrt{x+y^2}}\right)} - \frac{H(x,y)}{2y}\,. \tag{11}$$

Expressions (7) and (11) are valid for all values of $x \geq 0$ and $y > 1/2$.

Now, the decay constant, λ, is given by the product of three quantities, namely $\lambda = \lambda_0\,SP$, where

$$\lambda_0 = \frac{v}{2a} = \frac{\sqrt{2}}{2a}\sqrt{\frac{Q}{\mu_0}} \tag{12}$$

represents the number of assaults on the barrier per unit of time, and v is the relative velocity of the fragments.

The half-life of the decay process, $\tau = \log_{10} T_{1/2}$ [$T_{1/2}$ expressed in a (annum)] is thus obtained as

$$\tau = -29.5 + \log\left(a\sqrt{\frac{\mu_0}{Q}}\right) + (G_{\mathsf{ov}} + G_{\mathsf{sp}})\log(\mathrm{e}). \tag{13}$$

The observation that in cases of exotic decays for which $\ell \neq 0$ the quantity x is very small ($x \leq 2\times 10^{-3}$), the expansion of the functions $H(x,y)$ and $F(x,y)$ to first power of x suffices to take into account such a small effect in calculating half-lives. By introducing the new constant $u = 1/(2y)$, it results that

$$H(x,u) = \sqrt{\frac{1}{u} - 1} + \frac{x}{2\sqrt{\frac{1}{u} - 1}}\,, \tag{14}$$

$$F(x,u) = \arccos\sqrt{u} - \sqrt{u(1-u)}\cdot(1 - ux),\ x \geq 0,\ 0 < u < 1. \tag{15}$$

Finally, by expressing lengths in fm, masses in u, and energies in MeV, the decimal logarithm of the half-life (expressed in annum), $\tau_{\mathsf{e}} = \log T^{\mathsf{e}}_{1/2}(a)$, has been computed as

$$\tau_{\mathsf{e}} = -29.5 + \log\left(a\sqrt{\frac{\mu_0}{Q}}\right) + 0.19\, g_{\mathsf{se}}(c-a)\sqrt{\mu_0 Q}\cdot H(x,u) + 0.27358\, Z_{\mathsf{C}} Z_{\mathsf{D}}\sqrt{\frac{\mu_0}{Q}}\cdot F(x,u). \quad (16)$$

Accordingly, the unique, semiempirical parameter, g_{se}, of our half-life calculation ADLM can be evaluated as

$$g_{\mathsf{se}} = \alpha\cdot\tau_{\mathsf{e}} - \beta \quad (17)$$

where

$$\alpha = \frac{1}{0.19(c-a)\sqrt{\mu_0 Q}\cdot H(x,u)} \quad (18)$$

$$\beta = \alpha\left[-29.5 + \log\left(a\sqrt{\frac{\mu_0}{Q}}\right) + 0.27358\, Z_{\mathsf{C}} Z_{\mathsf{D}}\sqrt{\frac{\mu_0}{Q}}\cdot F(x,u)\right]. \quad (19)$$

For cluster decay cases for which $\ell = 0$ $(x = 0)$ the last two expressions reduced to

$$\alpha = \frac{1}{0.19\sqrt{\mu_0 Q}\,(c-a)\sqrt{(1-u)/u}} \quad (20)$$

$$\beta = \alpha\left\{-29.5 + \log\left(a\sqrt{\frac{\mu_0}{Q}}\right) + 0.27358\, Z_{\mathsf{C}} Z_{\mathsf{D}}\sqrt{\frac{\mu_0}{Q}}\left[\arccos\sqrt{u} - \sqrt{u(1-u)}\right]\right\}. \quad (21)$$

Note that the quantities α and β as given above identify unambiguously a certain case of cluster decay since both these quantities derive from values of $Z_{\mathsf{P,D,C}}$, $A_{\mathsf{P,D,C}}$, $R_{\mathsf{P,D,C}}$, the mass-excess values $\Delta M_{\mathsf{P,D,C}}$, and ℓ, this latter coming from the current nuclear spin ($\boldsymbol{J}$) and parity ($\boldsymbol{\pi}$) conservation laws. An uncertainty in the measured half-life, $\delta T^{\mathsf{e}}_{1/2}$, leads to an uncertainty in g_{se} of $\delta g_{\mathsf{se}} = \alpha(\delta T^{\mathsf{e}}_{1/2}/T^{\mathsf{e}}_{1/2})\log(\mathrm{e})$.

3 Basic input nuclear data

The application of the routine calculation ADLM to half-life evaluations of cases and modes of cluster emission from heavy nuclei requires knowledge of three basic quantities, *viz.* i) nuclear mass, ii) nuclear radius, and angular momentum associated with the ground-state to ground-state of the nuclear transition.

The values of both Q and μ_0 have been derived from the nuclear (rather than atomic) mass-values of the participating nuclides, namely

$$Q = m_{\mathsf{P}} - (m_{\mathsf{D}} + m_{\mathsf{C}}), \quad \mu_0 = \frac{m_{\mathsf{D}}\cdot m_{\mathsf{C}}}{m_{\mathsf{D}} + m_{\mathsf{C}}}, \quad (22)$$

where the m's are given by

$$m_i = A_i - Z_i\cdot m_{\mathsf{e}} + \frac{\Delta M_i + k\cdot Z_i^{\zeta}}{F}, \;\; i = \mathsf{P,\ D,\ C}, \quad (23)$$

in which $F = 931.4940038$ MeV/u is the mass-energy conversion factor, $m_{\mathsf{e}} = 0.5485799 \times 10^{-3}$ u is the electron rest mass, and ΔM is the atomic mass-excess values as tabulated by Wang *et al.* [51]. The quantity $k \cdot Z_i^{\zeta}$ represents the total binding energy of the Z_i electrons in the atom, where the values

$$\begin{aligned} k_1 &= 8.7 \times 10^{-6} \text{ MeV and } \zeta_1 = 2.517 \text{ for } Z \geq 60 \text{ and} \\ k_2 &= 13.6 \times 10^{-6} \text{ MeV and } \zeta_2 = 2.408 \text{ for } Z < 60 \end{aligned} \tag{24}$$

have been obtained from data reported by Huang *et al.* [55]. Thus, the Q-value for decay is calculated as

$$Q = \Delta M_{\mathsf{P}} - (\Delta M_{\mathsf{D}} + \Delta M_{\mathsf{C}}) + U, \tag{25}$$

$$U = k_1 \cdot (Z_{\mathsf{P}}^{\zeta_1} - Z_{\mathsf{D}}^{\zeta_1}) - k_2 \cdot Z_{\mathsf{C}}^{\zeta_2}. \tag{26}$$

U represents the effect of the screening to the nucleus caused by the surrounding electrons.

The nuclear-radius values, $R_i\,(i = \mathsf{P}, \mathsf{D}, \mathsf{C})$, have been evaluated following the finite range droplet model (FRDM) of atomic nuclei as described by Möller *et al.* [56], where the spherical approximation for the nuclear volume has been adopted (see also [57]). This nuclear radius parametrization has been updated by Möller *et al.* [53], who took into account more accurate experimental ground-state nuclear mass data. Accordingly, the expressions that enable to calculate the average equivalent root-mean-square radius-values of the proton and neutron density distributions are read as

$$R_i = \overline{Q}_{Z,A} = \frac{Z}{A} Q_{\mathsf{p}} + \left(1 - \frac{Z}{A}\right) Q_{\mathsf{n}},\ i = \mathsf{P}, \mathsf{D}, \mathsf{C}\,, \tag{27}$$

where the equivalent proton and neutron radii Q_j $(j = \mathsf{p}, \mathsf{n})$ are obtained from

$$Q_j = R_j \left(1 + \frac{5}{2R_j^2}\right). \tag{28}$$

Here, R_j denotes the sharp radii for proton and neutron density distributions, the values of which are given by

$$R_{\mathsf{p}} = r(1+\overline{\epsilon}) \left[1 - \frac{2}{3}\left(1 - \frac{Z}{A}\right)\left(1 - \frac{2Z}{A} - \overline{\delta}\right)\right] \cdot A^{1/3} \text{ and} \tag{29}$$

$$R_{\mathsf{n}} = r(1+\overline{\epsilon}) \left[1 + \frac{2}{3}\frac{Z}{A}\left(1 - \frac{2Z}{A} - \overline{\delta}\right)\right] \cdot A^{1/3}, \tag{30}$$

with $r = 1.16$ fm, and the values for the quantities $\overline{\epsilon}$ and $\overline{\delta}$ are given by [53]

$$\overline{\epsilon} = 0.854167 \exp\left(-0.988 A^{1/3}\right) - \frac{0.1896936}{A^{1/3}} + 0.2229167\,\overline{\delta} + 0.0031034 \frac{Z^2}{A^{4/3}} \text{ and} \tag{31}$$

$$\overline{\delta} = \frac{1 - \frac{2Z}{A} + 0.0048626 \frac{Z}{A^{2/3}}}{1 + 2.5304666 \frac{1}{A^{1/3}}}\,. \tag{32}$$

The evaluated reduced radius, $r_0 = R_i/A_i^{1/3} (i = \mathsf{P}, \mathsf{D}, \mathsf{C})$, of the equivalent liquid-drop-model for various nuclei is plotted in Fig. 2 as a function of mass number A. The trend reveals a strong decrease of reduced radius when one passes from less-massive nuclei to heavy ones, thus reflecting a clear degree of nuclear compressibility making, therefore, the simple formula $R = r_0 \cdot A^{1/3}$ not applicable to the entire range of mass number.

Finally, ℓ-values have been obtained from tabulated data on nuclear spin ($\boldsymbol{J}$) and parity ($\boldsymbol{\pi}$) compiled by Kondev *et al.* [52], by applying to them the usual conservation laws $\boldsymbol{J}_{\mathsf{P}} = \boldsymbol{J}_{\mathsf{D}} + \boldsymbol{J}_{\mathsf{C}} + \boldsymbol{\ell}$ and $\pi_{\mathsf{P}} = \pi_{\mathsf{D}} \cdot \pi_{\mathsf{C}} \cdot (-1)^{\ell}$.

4 Semiempirical determination of parameter g_{se}

The input half-life data for all experimentally known cases of exotic radioactivity measured for Th, Pa, U, Pu, and Cm parent isotopes by emission of Ne, Mg, and Si cluster isotopes have been taken from Refs. [24, 58–76]. In some cases there is a competitive emission between two cluster isotopes, for which cases it is known from the experiment only the total half-life of the decay processes, $\tau_{\mathsf{t}} = \log T_{1/2_{\mathsf{t}}}$, but not the partial half-life values for each emitted cluster isotope. This occurs for $^{234}\mathrm{U} \rightarrow {}^{24,26}\mathrm{Ne}$ [59, 61, 67, 68], $^{235}\mathrm{U} \rightarrow {}^{24,26}\mathrm{Ne}$ [61], $^{235}\mathrm{U} \rightarrow {}^{28,29}\mathrm{Mg}$ [70, 71], $^{236}\mathrm{U} \rightarrow {}^{28,30}\mathrm{Mg}$ [69], and $^{238}\mathrm{Pu} \rightarrow {}^{28,30}\mathrm{Mg}$ [24] emission cases.

If the assumption is made that both decay modes for the cases mentioned above are governed by the same semiempirical g_{se}-value, then following (17) one can write

$$g_{\mathsf{se}} = \alpha_1 \tau_1 - \beta_1 = \alpha_2 \tau_2 - \beta_2 \,, \tag{33}$$

where subscripts 1 and 2 refer to emitted clusters 1 and 2, respectively. The α's and β's can be known for each emitted cluster by using (18) and (19), and $\tau_i = \log T_{1/2_i}$ $(i = 1, 2)$ is the half-life for each decay mode. We want to find τ_i-values for the five decay cases cited above.

Here, by defining

$$f = \frac{\alpha_2}{\alpha_1}, \quad h = \frac{\beta_2 - \beta_1}{\alpha_1}, \quad m = 10^h, \tag{34}$$

we found that

$$\tau_2 = -\log(z) \quad \text{and} \quad \tau_1 = f \cdot \tau_2 - h, \tag{35}$$

where z is the solution of the equation

$$z + m \cdot z^f = \frac{1}{T_{1/2_{\mathsf{t}}}}. \tag{36}$$

Table 1 brings together input data on total measured half-life, $\tau_{\mathsf{e}} = \tau_{\mathsf{t}}$, α_i- and β_i-values $(i = 1, 2)$, as well as output results for τ_i and respective partial branching ratios values for the two modes of emitted cluster isotopes that were not identified in the five cases listed above.

In this way, we have collected thirty-four measured half-life values from nineteen identified exotic cluster decay cases. Firstly, it was evaluated $\overline{g}_{\mathsf{se}}$ and its uncertainty for each set of measurements of a

given exotic decay case [these are ^{230}U$\rightarrow^{22}$Ne (two measurements), ^{232}U$\rightarrow^{24}$Ne (five measurements), ^{234}U$\rightarrow^{24,26}$Ne and ^{234}U$\rightarrow^{28}$Mg (four measurements each)]. The uncertainty associated with each measured half-life has been considered to obtain a weighted, semiempirical $\overline{g}_{\mathsf{se}}$-parameter given by

$$\overline{g}_{\mathsf{se}} = \alpha \times \frac{\sum \frac{\tau_{\mathsf{e}_i}}{\delta\tau_{\mathsf{e}_i}^2}}{\sum \left(\frac{1}{\delta\tau_{\mathsf{e}_i}}\right)^2} - \beta, \quad \delta\overline{g}_{\mathsf{se}} = \frac{\alpha}{\sqrt{\sum \left(\frac{1}{\delta\tau_{\mathsf{e}_i}}\right)^2}} \,. \tag{37}$$

Table 2 lists such $\overline{g}_{\mathsf{se}}$ input data for the nineteen cases here examined.

Next, the "best" g_{se}-value which is applicable to all decay cases can be found by minimizing the quantity

$$D = \sqrt{\frac{\sum p_i \left(\tau_{\mathsf{c}_i} - \tau_{\mathsf{e}_i}\right)^2}{N}} \,, \; i = 1, \ldots, 19. \tag{38}$$

Here,

$$p_i = \frac{C}{\left(\delta\tau_{\mathsf{e}_i}\right)^2} \,, \quad \delta\tau_{\mathsf{e}_i} = \frac{\delta\overline{g}_i}{\alpha_i} \,, \tag{39}$$

$$\tau_{\mathsf{e}_i} = \frac{\overline{g}_i + \beta_i}{\alpha_i} \,, \quad \tau_{\mathsf{c}_i} = \frac{g + \beta_i}{\alpha_i} \,; \tag{40}$$

C is a normalization constant such that $\sum p_i = 1$, and τ_{c} and τ_{e} denote the decimal log of calculated and experimental half-lives, respectively. Introducing (39) and (40) into (38) one obtains

$$D = \sqrt{\frac{\sum p_i \left(\frac{g - \overline{g}_i}{\alpha_i}\right)^2}{N}} \,, \tag{41}$$

and after partial derivative with respect to g, $\partial D/\partial g = 0$, it gives

$$g \sum \frac{p_i}{\alpha_i^2} = \sum \frac{p_i\, \overline{g}_i}{\alpha_i^2} \,. \tag{42}$$

Finally, by using the relations (39) into (42) we get

$$g = \frac{\sum \frac{\overline{g}_i}{(\delta\overline{g}_i)^2}}{\sum \left(\frac{1}{\delta\overline{g}_i}\right)^2} \,, \quad \sigma_g = C \sum_{i=1}^{19} \frac{\alpha_i^2}{\delta\overline{g}_i} \,. \tag{43}$$

[for simplicity we have dropped the subscript se in (40)–(43)].
By using the $\overline{g}_i$-data of Table 2 into these two last results (43), one obtains

$$g \equiv g_{\mathsf{se}} = 0.3587 \pm 0.0009 \text{ (0.25\% uncertainty)}. \tag{44}$$

The g_{se}-value found in the present analysis is $\sim$2.78 % higher than that in our previous work ($g_{\mathsf{se}} =$ 0.3490 [13]) in view of the different sources for input data (nuclear mass and radius parametrization) as well as a different choice for exotic decay cases then analysed. Any way the use of a unique parameter in the calculation model (ADLM) has been sufficient to systematize the half-life data.

5 Half-life systematics of the exotic cluster decays considered in the present analysis

Once the g_{se}-value has been determined semiempirically the calculated half-lives, τ_{c}, can be obtained simply by evaluating

$$\tau_{\mathsf{c}} = \frac{g_{\mathsf{se}} + \beta}{\alpha}\,, \quad \delta\tau_{\mathsf{c}} = \frac{\delta g_{\mathsf{se}}}{\alpha}, \tag{45}$$

and the half-life itself given by

$$T^{\mathsf{c}}_{1/2} = 10^{\tau_{\mathsf{c}}}, \quad \delta T^{\mathsf{c}}_{1/2} = T^{\mathsf{c}}_{1/2} \cdot \delta\tau_{\mathsf{c}} \cdot \ln 10, \tag{46}$$

and the deviation of experimental- from calculated-value is $\Delta\tau = \tau_{\mathsf{c}} - \tau_{\mathsf{e}}$. Table 3 details a few examples of application of the present model to exotic decay cases showing a comparison between $T^{\mathsf{c}}_{1/2}$ and $T^{\mathsf{e}}_{1/2}$.

The data displayed in Table 3 cover a range of seven orders of magnitude in the half-life. It is seen that the knocking frequency against the barrier (λ_0, 2nd column) does not vary significantly, while the quantities S and P expand by five and nine orders of magnitude. The combination of these three quantities leads to the final calculated half-life value, which is comparable to the measured one. The last column indicates the ratio of calculated to experimental half-life results. The ratios are not greater than a factor 3, except for $^{231}\mathrm{Pa} \rightarrow {}^{24}\mathrm{Ne}$ decay case. This last one may be due to some loss of events during the experiments, or other causes that are difficult to identify.

The thirty-four half-life measurements collected in Table 2 have been compared with calculated values by our semiempirical, one-parameter ADLM as reported in the precedent sections. The distribution of the quantity $\Delta\tau = \tau_{\mathsf{c}} - \tau_{\mathsf{e}} = \log_{10}(T^{\mathsf{c}}_{1/2}/T^{\mathsf{e}}_{1/2})$ is shown in Fig. 3 (blue-line histogram). In constructing this $\Delta\tau$-distribution it has been found 26.5 % of the ratio $T^{\mathsf{c}}_{1/2}/T^{\mathsf{e}}_{1/2}$ (or its inverse) within a factor less than 2, 79.4 % within a factor less than 4, and only $\sim$ 20.6 % in the range $\sim$ 6–38. The biggest difference (a factor $\sim$ 39) between estimated and measured half-life values has been observed for $^{233}\mathrm{U} \rightarrow {}^{24}\mathrm{Ne} + {}^{209}\mathrm{Pb}$ decay case [65, 66].

The quality of the present results can be appreciated by looking at the red-line histogram displayed in Fig. 3. Such distribution has been obtained from data available from seventeen publications containing a total of four-hundred-one measured half-lives and their respective calculated ones by using different calculation models and parametrizations [22, 23, 29, 70, 77–89] for the same set of exotic decay cases that have been chosen in the present work. Four-hundred-one $\Delta\tau$-values have been thus extracted from the publications cited with which the red-line distribution in Fig. 3 has been constructed. This makes it clear about the suitability of a model of only one adjustable parameter with acceptable reproducing of measured half-life of exotic decays.

6 Searching for a simple dependence of half-life upon a quantity which characterizes the cluster decay case

The present one-parameter, semiempirical ADLM has been developed as a tunneling quantum mechanism through a potential barrier composed of an overlapping plus separation barrier regions, making it possible to estimate the half-lives of exotic cluster decay cases by means of simple expressions (45, 46), in which g_{se} is the semiempirical parameter of the model, and α and β are dimensionless quantities that identify the cluster decay case (see Eqs. (18–21)).

Looking at Fig. 1 and the adopted form for the potential energy in the overlapping region (Eq. (2)) the area of this region above the Q-value of the disintegration process is given by

$$\mathcal{A}_{\mathsf{ov}} = \frac{(V_c - Q)\cdot(c-a)}{q+1}, \quad V_c = \frac{Z_{\mathsf{C}} Z_{\mathsf{D}} e^2}{c} + \frac{\ell(\ell+1)\hbar^2}{2\mu_0 c^2}\,. \tag{47}$$

For radioactive decays by cluster emission the term containing $\ell(\ell+1)$ can be considered null or negligible, thus

$$\mathcal{A}_{\mathsf{ov}} = \left(\frac{Z_{\mathsf{C}} Z_{\mathsf{D}} e^2}{c} - Q\right)\frac{c-a}{q+1}\,. \tag{48}$$

Now, the area of the separation region ($c-b$ in Fig. 1) above the Q-value is calculated as

$$\mathcal{A}_{\mathsf{sp}} = Z_{\mathsf{C}} Z_{\mathsf{D}} e^2 \ln\left(\frac{b}{c}\right) + \frac{\ell(\ell+1)\hbar^2}{2\mu_0}\cdot\left(\frac{1}{c} - \frac{1}{b}\right) - Q(b-c), \tag{49}$$

and since the second term in this expression is negligible in view of the other ones, (49) transforms to

$$\mathcal{A}_{\mathsf{sp}} = cQ - Z_{\mathsf{C}} Z_{\mathsf{D}} e^2 (1 + \ln(u)), \quad u = \frac{cQ}{Z_{\mathsf{C}} Z_{\mathsf{D}} e^2}\,. \tag{50}$$

By summing up (48) and (50) the total area between $V(s)$ and Q-value in the interval $a \le s \le b$ is given by

$$\mathcal{A}_{\mathsf{T}} = Q\cdot\left\{(c-a)\cdot\frac{u^{-1}-1}{q+1} + c\left[1 - \frac{1+\ln(u)}{u}\right]\right\}. \tag{51}$$

Based on preliminary calculation of $\mathcal{A}_{\mathsf{T}}$-values by using (51) we have found out an increasing, rather linear dependence of τ upon $\mathcal{A}_{\mathsf{T}}$ when parameter q is put equal to $1/u$. Therefore, it results

$$\mathcal{A}_{\mathsf{T}} = Q\left\{(c-a)\cdot\frac{1-u}{1+u} + c\left[1 - \frac{1+\ln(u)}{u}\right]\right\}. \tag{52}$$

Such a dependence τ *vs* $\mathcal{A}_{\mathsf{T}}$ can be appreciated in Fig. 4 for the nineteen cluster decay cases examined in the present work plus five new predicted emission clusters from ^{238}U and ^{232}Th parent nuclei (part a) of Fig. 4). Part b) shows the same dependence for the experimentally determined τ_{e}-values. Note that the quantity y (second expression in (5)) contains all quantities involved in a cluster decay case, *viz.* i) the atomic numbers of the decay products ($Z_{\mathsf{C}}, Z_{\mathsf{D}}$), the Q-value of the decay process, and the nuclear radii of the participating nuclides through $c - a = 2R_{\mathsf{C}} - (R_{\mathsf{P}} - R_{\mathsf{D}})$. In this way $\mathcal{A}_{\mathsf{T}}$ (expressed in MeV$\cdot$ fm) characterizes alternatively a given cluster decay case.

The fact that $q = 1/u$ leads to a good linear correlation τ *vs* $\mathcal{A}_{\mathsf{T}}$ allows one to obtain information about the values of the exponent p in the power form expression supposed to describe the reduced mass of the decaying system in the overlapping barrier region (see Eq. (1)) and, therefore, the spectroscopic factor $S = \exp(-G_{\mathsf{ov}})$. According to Eq. (8), g_{se} comes from a combination of exponents p and q in such a way that $g_{\mathsf{se}} = [(p+q)/2+1]^{-1}$. By using the value $g_{\mathsf{se}} = 0.3587$ found in the present analysis one arrives at

$$p = 3.5757 - q\,. \tag{53}$$

Since for the cluster decay processes considered in the present study $0.53 \leq u \leq 0.68$ (see Table 4) it follows that $1.47 \leq q \leq 1.89$ and $1.7 \leq p \leq 2.1$, which means that both functions $\mu(s)$ and $V(s)$ in the overlapping barrier region ($a \leq s \leq c$) are power functions concave upward.

7 Final remarks and conclusion

In the same way as occurs in α-decay and fission processes, the radioactive decay of heavy nuclei by the emission of fragments heavier than the α-particle is governed by the nuclear shell structure where the most probable decay cases observed (and predicted) to date take place when the produced nuclides exhibit neutron or proton shell closure, mainly the double magic ^{208}Pb daughter isotope or their neighbor nuclides, a fact demonstrated for just over forty years or so. Here, the phenomenon has been treated like the α-decay process, *i.e.*, a quantum tunneling mechanism of penetration through a potential barrier to evaluate the partial half-lives of a number of cases, *viz.* spontaneous emission of C–Si isotopes from beyond lead parent isotopes.

A semiempirical, one-parameter calculation model to predict half-life values of these radioactive processes has been introduced in 2005 to explain the rare alpha activity observed in until then considered stable ^{209}Bi isotope ($\sim 3.3\,\mu$Bq/g of bismuth) [41]. Later on, this model (here named "alpha-decay like model" —ADLM) was applied successfully in a number of α-decay cases, one- and two-proton emission cases, and notably in the exotic cluster decay cases [13].

The available, updated atomic mass-excess- and nuclear-radius values led us to apply the present ADLM to a half-life re-evaluating of radioactive decay of Th, Pa, U, Pu, and Cm isotopes by the emission of Ne, Mg, and Si isotopes. The usage of nuclear (rather than atomic) mass values enables us to obtain more reliable estimates of both Q-value and reduced-mass value, μ_0, of the decay processes. The same happens from an updating of nuclear radius parametrization [53] as compared with the previous one [56] that had been used in our precedent analysis [13]. The radius values resulting from the updated FRDM of atomic nuclei as reported in [53] give a better description for both the overlapping and separation barrier regions.

By considering a unique g_{se}-value for the parameter of the model it has been possible to obtain the branching ratios for each cluster emitted in a few cases where the competitive emission between two cluster isotopes had not been resolved experimentally, such as for instance in the $^{234}\mathrm{U} \rightarrow {}^{24,26}\mathrm{Ne}$

radioactive decay. All together nineteen exotic decay cases involving the emission of ^{22,24,26}Ne, $^{28-30}$Mg, and ^{32,34}Si cluster isotopes, and ^{230}Th, ^{231}Pa, $^{230,232-236}$U, ^{236,238}Pu, and ^{242}Cm parent emitter isotopes, totalizing thirty-four half-life measurements, have been systematically analyzed (some selected decay cases are presented in Table 3). Agreement of calculated half-life values with the measured ones can be considered very satisfactory in view of the difficulties inherent to the decay process itself (poor statistics, unfavorable competition with α-decay) and yet uncertainties associated to nuclear quantities. Even so, $\sim 80\,\%$ of the measured half-life measurements have been reproduced within a factor less than 4. Moreover, the quality of the present systematic analysis can be appreciated by looking at the two $\Delta\tau = \log_{10}(T^{\mathsf{c}}_{1/2}/T^{\mathsf{e}}_{1/2})$ distributions depicted in Fig. 3. It is seen a clear narrowness of the present $\Delta\tau$-distribution as compared with that of four-hundred-one $\Delta\tau$-values from different models and/or parametrizations for the same decay cases considered in the present work.

The ADLM model as described in the previous sections relies on the premise that there is a single, semiempirical, adjustable parameter, g_{se}, with which it is possible to reproduce the measured half-lives of a set of cases of exotic radioactivity. Such a parameter describes in a semiempirical way the overlapping region of the nascent fragments in the process of preforming the cluster to be emitted through a potential barrier.

Since g_{se} results from a combination of two exponents, p and q, which define the power functions adopted for the reduced mass and potential barrier, respectively, in the overlapping region, $g_{\mathsf{se}} = 1/[(p+q)/2+1]$, we carried out a search for information on values of p and q. We then have discovered a fairly linear correlation between $\tau = \log T_{1/2}$ and the area, $\mathcal{A}_{\mathsf{T}}$, of the region bounded by the potential energy curve and the Q-value line (constant) across the entire barrier region (overlapping plus separation) when q has been put equal to $1/u$, *i.e.* $q = 1/u = Z_{\mathsf{C}} Z_{\mathsf{D}}\, e^2/(c\,Q)$ (Fig. 4). Therefore, with the semiempirical value $g_{\mathsf{se}} = 0.3587$ found from the ADLM calculations, one arrives at $p = 3.5757 - q$. Thus, for the exotic decay cases considered in the present study, one has $1.47 \leq q \leq 1.87$ and $1.70 \leq p \leq 2.11$, meaning that both the $\mu(s)$ and $V(s)$ curves are concave upwards in the region where the cluster and product nuclide are formed.

To conclude, the present ADLM methodology has proved capable of reliably reproduce the half-lives of exotic radioactive decays with mass asymmetry of the disintegrating products, $\eta = (A_{\mathsf{D}} - A_{\mathsf{C}})/A_{\mathsf{P}}$, for cases in which $0.71 \leq \eta \leq 0.81$. The model can also be applied to emission of clusters of lower atomic number and/or mass number (^{14}C, ^{20}O, ^{23}F) for which $0.80 \leq \eta \leq 0.88$. In α-decay, systematics of half-life can be constructed for isotopic sequences of heavy and superheavy nuclei. The model can also be useful in investigating of the fine structure of alpha spectra of ground state α-emitters, and also to predict alpha emission half-lives of nuclei in isomeric states.

References

[1] H. G. de Carvalho, J. B. Martins, I. O. de Souza, O. A. P. Tavares, Emissão espontânea de íons pesados pelo urânio (Spontaneous emission of heavy ions from uranium). An. Acad. Brasil. Ciênc. **47**, 567 (1975); Chem. Abstr. **85**, 441 (1976) (entry no. 85:100326j).

[2] H. G. de Carvalho, J. B. Martins, I. O. de Souza, O. A. P. Tavares, Emissão espontânea de íons pesados pelo urânio (Spontaneous emission of heavy ions from uranium). An. Acad. Brasil. Ciênc. **48**, 205 (1976).

[3] I. O. de Souza, Meia-vida de fissão espontânea do ^{238}U e uma provável nova forma de radioatividade (Spontaneous fission half-life of Uranium-238 and a probable new type of radioactivity). MSc Thesis, Centro Brasileiro de Pesquisas Físicas-CBPF (Rio de Janeiro, 1975).

[4] O. A. P. Tavares, Alta assimetria de massa na desintegração espontânea e induzida de núcleos pesados (High mass asymmetry in spontaneous and induced disintegrations of heavy nuclei). Doctoral Thesis, Centro Brasileiro de Pesquisas Físicas-CBPF (Rio de Janeiro, 1978).

[5] D. N. Poenaru, M. Ivascu, A. Sandulescu, W. Greiner, Spontaneous emission of heavy clusters. J. Phys. G: Nucl. Part. Phys. **10**, L183 (1984).

[6] D. N. Poenaru, M. Ivascu, A. Sandulescu, W. Greiner, Atomic nuclei decay modes by spontaneous emission of heavy ions. Phys. Rev. C **32**, 572 (1985).

[7] D. N. Poenaru, W. Greiner, K. Depta, M. Ivascu, D. Mazilu and A. Sandulescu, Calculated half-lives and kinetic energies for spontaneous emission of heavy ions from nuclei. At. Data Nucl. Data Tables **34**, 423 (1986).

[8] A. Sandulescu, W. Greiner, Mass asymmetry in fission, fusion and mass-transfer due to fragmentation in valleys. J. Phys. G: Nucl. Part. Phys. **3**, L189 (1977).

[9] A. Sandulescu, M. J. Lustig. J. Hahn, W. Greiner, High mass-asymmetry distributions of fissioning nuclei. J. Phys. G: Nucl. Part. Phys. **41**, 279 (1978).

[10] A. Sandulescu, D. N. Poenaru, W. Greiner, New type of decay of heavy nuclei intermediate between fission and α decay. Fiz. Elem. Chastits At. Yadra **11**, 1334 (1980) [Sov. J. Part. Nucl. **11**, 528 (1980)].

[11] H. G. de Carvalho, J. B. Martins, O. A. P. Tavares, Radioactive decay of radium and radon isotopes by ^{14}C emission. Phys. Rev. C **54**, 2261 (1986).

[12] O. A. P. Tavares, L. A. M. Roberto, E. L. Medeiros, Radioactive decay by the emission of heavy nuclear fragments. Phys. Scr. **76**, 375 (2007).

[13] O. A. P. Tavares, E. L. Medeiros, A simple description of cluster radioactivity. Phys. Scr. **86**, 015201 (2012).

[14] H. J. Rose, G. A. Jones, A new kind of natural radioactivity. Nature (London) **307**, 245 (1984).

[15] D. V. Aleksandrov, A. F. Belyatskii, Yu. A. Glukhov, E. Yu. Nikolskii, B. G. Novatskii, A. A. Oglobin, D. N. Stepanov, Observation of the spontaneous emission of ^{14}C nuclei from ^{223}Ra. Pis. Zh. Eksp. Teor. Fiz. **40**, 152 (1984) [Sov. Phys. — JETP Lett. **40**, 909 (1984)].

[16] S. Gales, E. Hourani, M. Hussonnois, J. P. Schapira, L. Stab, M. Vergnes, Exotic nuclear decay of ^{223}Ra by emission of ^{14}C nuclei. Phys. Rev. Lett. **53**, 759 (1984).

[17] P. B. Price, J. D. Stevenson, S. W. Barwick, H. L. Ravn, Discovery of radioactive decay of ^{222}Ra and ^{223}Ra by ^{14}C emission. Phys. Rev. Lett. **54**, 297 (1985).

[18] W. Kutschera, I. Ahmad, S. G. Armato III, A. M. Friedman, J. E. Gindler, W. Henning, T. Ishic, M. Paul, K. E. Rhem, Spontaneous ^{14}C emission from ^{223}Ra. Phys. Rev. Lett. **32**, 2036 (1985).

[19] L. Brillard, A. G. Elayi, E. Hourani, M. Hussonnois, J. F. Le Du, L. H. Rosin, L. Stab, Evidence for a fine structure in ^{14}C radioactivity. C. R. Acad. Sci. (Paris) **309**, 1105 (1989).

[20] E. Hourani, L. Rosier, G. Berrier-Ronsin, A. Elayi, A. C. Mueller, G. Rappenecker, G. Rotbard, G. Renou, A. Libe, L. Stab, H. L. Ravn, Fine structure in ^{14}C emission from ^{223}Ra and ^{224}Ra. Phys. Rev. C **44**, 1424 (1991).

[21] D. N. Poenaru, R. A. Gherghescu, Cluster radioactivity, J. Nucl. Phys. Mat. Sci. Rad. A **8**, 65 (2020).

[22] Y. Wang, F. Xing, Y. Xiao, J. Gu, An improved semi-empirical relationship for cluster radioactivity, Chin. Phys. C **45**, 044111 (2021).

[23] K. P. Santhosh, V. K. Anjali, Cluster radioactivity using modified generalized liquid drop model with a statistical cluster preformation probability, Nucl. Phys. A **1041**, 122787 (2024).

[24] S. Wang, D. Snowden-Ifft, P. B. Price, K. J. Moody, E. K. Hulet, Heavy fragment radioactivity of ^{238}Pu: Si and Mg emission. Phys. Rev. C **39**, 1647 (1989).

[25] Yu. S. Zamyatnin, V. L. Mikheev, S. P. Tretyakova, V. I. Furman, S. G. Kadmenskii, Yu. M. Chuvilskii, Cluster radioactive: Progress and perspectives; experimental and theory, Sov. J. Part. Nucl. **21**, 231 (1990).

[26] M. Gonçalves, S. B. Duarte, Effective liquid drop description for exotic decay of nuclei, Phys. Rev. C **48**, 2409 (1993).

[27] D. N. Poenaru (Ed.), Nuclear Decay Modes (Bristol: Institute of Physics Publishing) chapters 6–9 (1996).

[28] S. P. Tretyakova, A. A. Ogloblin, G. A. Pik-Pichak, The present state of cluster radioactivity research, Phys. Atom. Nucl. **66**, 1618 (2003).

[29] S. N. Kuklin, G. G. Adamian, N. V. Antonenko, Spectroscopic factors and cluster half-lives of heavy nuclei, Phys. Rev. C **71**, 014301 (2005).

[30] E. Hourani, M. Hussonnois, D. N. Poenaru, Radioactivities by light fragments (C, Ne, Mg) emission, Ann. Phys. (Paris) **14**, 311 (1989).

[31] D. N. Poenaru, W. Greiner, Cluster Radioactivity, in Lecture Notes in Physics, Christian Beck Ed., vol. **818**. Clusters in Nuclei (Springer, 2010), pp. 1–56.

[32] Y. Ronen, Significance of the light clusters in exotic nuclear decay, Phys. Rev. C **44**, R594 (1991).

[33] D. Ni, Z. Ren, T. Dong, C. Xu, Unified formula of half-lives for α decay and cluster radioactivity. Phys. Rev. C **78**, 044310 (2008).

[34] D. N. Poenaru, R. A. Gerghescu, W. Greiner, Single universal curve for cluster radioactivities, Phys. Rev. C **83**, 014601 (2011).

[35] D. N. Poenaru, R. A. Gerghescu, W. Greiner, Cluster decay of superheavy nuclei. Phys. Rev. C **85**, 034615 (2012).

[36] Y. L. Zhang, Y. Z. Wang, Systematic study of cluster radioactivity of superheavy nuclei. Phys. Rev. C **97**, 014318 (2018).

[37] M. Warda, A. Zdeb, L. M. Robledo, Cluster radioactivity in superheavy nuclei. Phys. Rev. C **98**, 041602 (2018).

[38] P. de Marcillac, N. Coron, G. Dambier, J. Leblanc, J. P. Moalic, Experimental detection of α-particles from radioactive decay of natural bismuth. Nature **422**, 876 (2003).

[39] G. Gamow, Zur quantentheory des atomkernes, Z. Phys. **51**, 204 (1928).

[40] R. W. Gurney, E. U. Condon, Wave Mechanics and Radioactive Disintegration, Nature **122**, 439 (1928). Quantum Mechanics and Radioactive Disintegration, Phys. Rev. **33**, 127 (1929).

[41] O. A. P. Tavares, E. L. Medeiros, M. L. Terranova, Alpha decay half-life of bismuth isotopes, J. Phys. G: Nucl. Part. Phys. **31**, 129 (2005).

[42] O. A. P. Tavares, M. L. Terranova, E. L. Medeiros, New evaluation of alpha decay half-life of ^{190}Pt isotope for Pt-Os dating system, Nucl. Instrum. Methods Phys. Res. B **243**, 256 (2006).

[43] E. L. Medeiros, M. M. N. Rodrigues, S. B. Duarte, O. A. P. Tavares, Systematics of alpha decay half-life: new evaluation of alpha emitter nuclides, J. Phys. G: Nucl. Part. Phys. **32**, B23 (2006).

[44] E. L. Medeiros, M. M. N. Rodrigues, S. B. Duarte, O. A. P. Tavares, Systematics of half-lives for proton radioactivity, Eur. Phys. J. A **34**, 417 (2007).

[45] O. A. P. Tavares, M. L. Terranova, Partial alpha-decay half-lives for alpha-emitting Osmium isotopes: Accurate determinations by a semi-empirical model, Appl. Radiat. Isot. **160**, 109034 (2020).

[46] O. A. P. Tavares, E. L. Medeiros, M. L. Terranova, Alpha-decay half-life of Hafnium isotopes reinvestigated by a semi-empirical approach, Appl. Radiat. Isot. **166**, 109381 (2020).

[47] O. A. P. Tavares, M. L. Terranova, Toward an accurate determination of half-life of ^{147}Sm Isotope, Appl. Radiat. Isot. **139**, 26 (2018).

[48] O. A. P. Tavares, M. L. Terranova, A semiempirical evaluation of half-life of ^{146}Sm isotope, Mod. Phys. Lett. A **38**, 2350115 (2023).

[49] O. A. P. Tavares, E. L. Medeiros, M. L. Terranova, Partial alpha-decay half-life of ^{178}Hf^{m2} isomer, Mod. Phys. Lett. A **36**, 2150036 (2021).

[50] O. A. P. Tavares, E. L. Medeiros, A calculation model to half-life estimate of two-proton radioactive decay process, Eur. Phys. J. A **54**, 65 (2018).

[51] M. Wang, W. J. Huang, F. G. Kondev, G. Audi and S. Naimi, The AME2020 atomic mass evaluation (II). Tables, graphs, and references. Chin. Phys. C **45**, 030003 (2021).

[52] F. G. Kondev, M. Wang, W. J. Huang, S. Naimi and G. Audi, The NUBASE2020 evaluation of nuclear physics properties, Chin. Phys. C **41**, 030001 (2021).

[53] P. Möller, A. J. Sierk, T. Ichikawa, H. Sagawa, Nuclear ground-state masses and deformations: FRDM (2012), At. Data Nucl. Data Tables **109–110**, 1 (2016).

[54] S. B. Duarte, M. G. Gonçalves, Effective inertial coefficient for the dinuclear regime of the exotic decay of nuclei, Phys. Rev. C **53**, 2309 (1996).

[55] K.-N. Huang, M. Aoyagi, M. H. Chen, B. Crasemann, H. Mark, Neutral-atom electron binding energies from relaxed-orbital relativistic Hartree-Fock-Slater calculations $2 \leq Z \leq 106$, At. Data Nucl. Data Tables **18**, 243 (1976).

[56] P. Möller, J. R. Nix, W. D. Myers, W. J. Swiatecki, Nuclear ground-state masses and deformations, At. Data Nucl. Data Tables **59**, 185 (1995).

[57] W. D. Myers, Droplet Model of Atomic Nuclei (New York, Plenum, 1977).

[58] R. Bonetti, C. Carbonini, A. Guglielmetti, M. Hussonnois, D. Trubert, C. Le Naour, Cluster decay of ^{230}U via Ne emission, Nucl. Phys. A **686**, 64 (2001).

[59] K. J. Moody, E. K. Hulet, S. Wang, P. B. Price, Heavy-fragment radioactivity of ^{234}U, Phys. Rev. C **39**, 2445 (1989).

[60] Q. Pan, W. Yang, S. Yuan, Z. Li, T. Ma, Y. Luo, D. Kong, J. Qiao, Z. Luo, M. Zhang, S. Wang, Search for heavy ion emission from the decay of ^{230}U, Phys. Rev. C **62**, 044612 (2000).

[61] R. Bonetti, C. Chiesa, A. Guglielmetti, C. Migliorino, A. Cesana, M. Terrani, P. B. Price, Neon radioactivity of uranium isotopes. Phys. Rev. C **44**, 888 (1991).

[62] S. W. Barwick, P. B. Price, J. D. Stevenson, Radioactive decay of ^{232}U by ^{24}Ne emission. Phys. Rev. C **31**, 1984 (R) (1985).

[63] R. Bonetti, E. Fioretto, C. Migliorino, A. Pasinetti, F. Barranco, E. Vigezzi, Revising the Chart of the Nuclides by exotic decay. Phys. Lett. B **241**, 179 (1990).

[64] R. Bonetti and A. Guglielmetti, Cluster radioactivity: An overview after twenty years. Roman. Rep. Phys. **59**, 301 (2007).

[65] S. P. Tretyakova, A. Sandulescu, Yu. S. Zamyatnin, Yu. S. Kovotkin, V. L. Mikheev, Emission of Ne ions by ^{233}U decay. JINR Rapid Commn. **7**, 23 (1985).

[66] P. B. Price, K. J. Moody, E. K. Hulet, R. Bonetti, C. Migliorino, High-statistics study of cluster radioactivity from ^{233}U. Phys. Rev. C **43**, 1781 (1991).

[67] S. Wang, P. B. Price, S. W. Barwick, K. J. Moody, E. K. Hulet, Radioactive decay of ^{234}U via Ne and Mg emission. Phys. Rev. C **36**, 2717 (1987).

[68] S. P. Tretyakova, Yu. S. Zamyatnin, V. N. Kovantsev, Yu. Korotkin, V. I. Mikheev, G. A. Timofeev, Observation of nucleon clusters in the spontaneous decay of ^{234}U. Z. Phys. A (Atomic Nuclei) **333**, 349 (1989).

[69] S. P. Tretyakova, V. L. Mikheev, V. A. Ponomarenko, A. N. Golovchenko, A. A. Ogloblin, V. A. Shigin, Cluster decay of ^{236}U. JETP Lett. **59**, 394 (1994).

[70] Z. Wang, Z. Ren, Effects of nuclear surface polarization on exotic cluster radioactivity in trans-lead nuclei. Phys. Rev. C **108**, 024306 (2023).

[71] N. Ashok, M. Rohith, Exotic decay modes of uranium isotopes. Nucl. Phys. A **1037**, 122686 (2023).

[72] A. A. Ogloblin, N. I. Venikov, S. K. Lisin, S. V. Pirozhkov, V. A. Pchlin, Yu. F. Rodionev *et al.*, Detection of radioactive ^{236}Pu decay with emission of ^{28}Mg nuclei. Phys. Lett. B **235**, 35 (1990).

[73] S. P. Tretyakova, A. Sandulescu, V. L. Mikheev, D. Hasegan, I. A. Lebedev, Yu. S. Zamyatnin, Yu. S. Kovotkin, B. F. Myasoedov, On the spontaneous emission of clusters by the ^{230}Th, ^{237}Np, and ^{241}Am nuclei. JINR Rapid Commun. **13**, 34 (1985).

[74] P. B. Price, R. Bonetti, A. Guglielmetti, C. Chiesa, R. Matheoud, C. Migliorino, K. J. Moody, Emission of ^{23}F and ^{24}Ne in cluster radioactivity of ^{231}Pa. Phys. Rev. C **46**, 1939 (1992).

[75] A. A. Ogloblin, R. Bonetti, V. A. Denisov, A. Guglielmetti, M. G. Itkis, C. Mazzocchi *et al.*, Observation of cluster decay of ^{242}Cm. Phys. Rev. C **61**, 034301(2000).

[76] S. P. Tretyakov, R. Bonetti, A. Golovchenko, A. Guglielmetti, R. Ilic, Ch. Mazzocchi, Study of cluster decay of ^{242}Cm using SSNTD. Radiat. Measur. **34**, 241 (2001).

[77] K. P. Santhosh, B. Priyanka, M. S. Unnikrisman, Cluster decay half-lives of trans-lead nuclei within the Coulomb and proximity potential model. Nucl. Phys. A **889**, 29 (2012).

[78] L.- J. Qi, D.- M. Zhang, S. Luo, X.- H. Li, X.- J. Wu, C.- T. Liang, Systematic calculation of cluster radioactivity half-lives in trans-lead nuclei. Chin. Phys. C **47**, 014101 (2023).

[79] S. B. Duarte, O. A. P. Tavares, F. Guzmán, A. Dimarco, F. García, O. Rodríguez, M. Gonçalves, Half-lives for proton emission, alpha decay, cluster radioactivity and cold fission processes calculated in a unified theoretical framework. At. Data Nucl. Data Tables **80**, 235 (2002).

[80] G. Royer, R. Moustabchir, Light nucleus emission within a generalized liquid-drop model and quasimolecular shapes. Nucl. Phys. A **683**, 182 (2001).

[81] W. M. Seif, L. H. Hamer, Systematic investigation of cluster radioactivity for uranium isotopes. Nucl. Phys. A **969**, 254 (2018).

[82] A. Jain, P. K. Sharma, S. K. Jain, J. K. Deegwal, G. Saxena, Cluster radioactivity in trans-lead region: A systematic study with modified empirical formulas. Nucl. Phys. A **1031**, 122597 (2023).

[83] A. Soylu, C. Qi, Extended universal decay law formula for the α and cluster decays. Nucl. Phys. A **1013**, 122221 (2021).

[84] M. Horoi, Scaling behavior in cluster decay. J. Phys. G: Nucl. Part. Phys. **30**, 945 (2004).

[85] M. Balasubramaniam, S. Kumarasamy, N. Arunachalan, R. K. Gupta, New semiempirical formula for exotic cluster decay. Phys. Rev. C **70**, 017301 (2004).

[86] C. Qi, F. R. Xu, R. J. Liotta, R. Wyss, M. Y. Zhang, C. Asawatangtrakuldee, D. Hu, Microscopic mechanism of charged-particle radioactivity and generalization of the Geiger-Nuttall law. Phys. Rev. C **80**, 044326 (2009).

[87] M. Ismail, A. Y. Ellithi, A. Adel, M. A. Abbas, An improved unified formula for α-decay and cluster radioactivity of heavy and superheavy nuclei. Eur. Phys. J. A **58**, 225 (2022).

[88] M. R. Pahlavani, S. Rahimi Shamami, Cluster decay half-life of various heavy deformed nuclei with mass numbers in the range $221 \leq A \leq 242$. Chin. J. Phys. **66**, 723 (2020).

[89] D. N. Poenaru, W. Greiner, Cluster radioactivities —Past, present and future. Int. J. Mod. Phys. E **17**, 2255 (2008).

Table 1 - Half-life values of each emitted cluster in cases of exotic decays by two experimentally unidentified cluster isotopes.

Decay case	Ref.	$\tau_e = \log_{10} T^e_{1/2}$[a]	α_2	β_2	α_1	β_1	τ_2	branching ratio (%)	τ_1	branching ratio (%)
^{234}U $\rightarrow$ ^{24,26}Ne	68	17.7993 ± 0.1172	0.0213	0.0292	0.0205	0.0277	17.8909	81.0, ^{24}Ne	18.5204	19.0, ^{26}Ne
	67	17.5682 ± 0.1174					17.6615	80.7, ^{24}Ne	18.2819	19.3, ^{26}Ne
	61	18.4330 ± 0.3157					18.5199	81.8, ^{24}Ne	19.1741	18.1, ^{26}Ne
	59	17.7506 ± 0.050					17.8425	80.9, ^{24}Ne	18.4701	19.1, ^{26}Ne
^{235}U $\rightarrow$ ^{24,26}Ne	61	19.9410 ± 0.2328	0.0210	0.0719	0.0202	0.0663	20.0613	75.8, ^{24}Ne	20.5574	24.2, ^{26}Ne
^{235}U $\rightarrow$ ^{28,29}Mg	70	19.9448	0.0187	0.0162	0.0184	0.0210	20.0340	81.4, ^{28}Mg	20.6763	18.6, ^{29}Mg
^{236}U $\rightarrow$ ^{28,30}Mg	69	20.0792	0.0184	0.0545	0.0180	0.0293	21.0437	10.9, ^{28}Mg	20.1318	89.1, ^{30}Mg
^{238}Pu $\rightarrow$ ^{28,30}Mg	24	18.1931 ± 0.1642	0.0189	-0.0182	0.0183	-0.0262	18.4465	55.8, ^{28}Mg	18.5477	44.2, ^{30}Mg

Table 2 - Experimental decay data for the determination of semiempirical parameter of the present model ($g_{\mathsf{se}} \pm \delta g_{\mathsf{se}}$)[a].

No.	Decay case	α	β	$\tau_{\mathsf{e}} \pm \delta\tau_{\mathsf{e}}$	$(\overline{g}_{\mathsf{se}} \pm \delta\overline{g}_{\mathsf{se}})$[b]	Ref.
1	^{230}Th $\rightarrow$ ^{24}Ne	0.021580	0.015215	17.1303 ± 0.0772	0.3544 ± 0.0017	73
2	^{231}Pa $\rightarrow$ ^{24}Ne	0.021934	-0.038511	15.3874 ± 0.0552	0.3760 ± 0.0012	74
3	^{230}U $\rightarrow$ ^{22}Ne	0.022930	-0.060226	12.0622 ± 0.181	0.3409 ± 0.0034	58
4				12.6295 ± 0.2671		60
5	^{232}U $\rightarrow$ ^{24}Ne	0.022117	-0.068991	12.8898 ± 0.0348	0.3547 ± 0.0004	61
6				13.5372 ± 0.1085		62
7				12.9071 ± 0.0367		63
8				12.8762 ± 0.0520		64
9				12.8997 ± 0.0466		64
10	^{233}U $\rightarrow$ ^{24}Ne	0.021662	-0.017404	17.3446 ± 0.0603	0.3930 ± 0.0012	66
11				17.3268 ± 0.1445		65
12	^{234}U $\rightarrow$ ^{24}Ne	0.021293	0.029245	17.8909 ± 0.1172	0.3506 ± 0.0012	68
13				17.6615 ± 0.1174		67
14				18.5199 ± 0.3157		61
15				17.8425 ± 0.0498		59
16	^{234}U $\rightarrow$ ^{26}Ne	0.020488	0.027733	18.5204 ± 0.1172	0.3506 ± 0.0012	68
17				18.2820 ± 0.1174		67
18				19.1742 ± 0.3157		61
19				18.4701 ± 0.0498		59
20	^{234}U $\rightarrow$ ^{28}Mg	0.019046	-0.021352	18.2502 ± 0.0786	0.3674 ± 0.0012	64
21				18.0282 ± 0.1323		64
22				18.0414 ± 0.5527		67
23				18.0414 ± 0.1579		68
24	^{235}U $\rightarrow$ ^{24}Ne	0.020976	0.071865	20.0613 ± 0.2328	0.3489 ± 0.0049	61
25	^{235}U $\rightarrow$ ^{26}Ne	0.020198	0.066272	20.5574 ± 0.2328	0.3489 ± 0.0047	61
26	^{235}U $\rightarrow$ ^{28}Mg	0.018731	0.016246	20.0340 ± 0.2583	0.3590 ± 0.0048	70, 71
27	^{235}U $\rightarrow$ ^{29}Mg	0.018381	0.021030	20.6763 ± 0.2587	0.3590 ± 0.0047	70, 71
28	^{236}U $\rightarrow$ ^{28}Mg	0.018429	0.054465	21.0437 ± 0.2328	0.3334 ± 0.0043	69
29	^{236}U $\rightarrow$ ^{30}Mg	0.018017	0.029322	20.1318 ± 0.2328	0.3334 ± 0.0042	69
30	^{236}Pu $\rightarrow$ ^{28}Mg	0.019613	-0.098276	14.1761 ± 0.2895	0.3763 ± 0.0057	72
31	^{238}Pu $\rightarrow$ ^{28}Mg	0.018867	-0.018221	18.4465 ± 0.1665	0.3662 ± 0.0031	24
32	^{238}Pu $\rightarrow$ ^{30}Mg	0.018335	-0.026191	18.5477 ± 0.1665	0.3662 ± 0.0030	24
33	^{238}Pu $\rightarrow$ ^{32}Si	0.017235	-0.053325	17.8028 ± 0.2257	0.3601 ± 0.0039	24
34	^{242}Cm $\rightarrow$ ^{34}Si	0.017085	-0.097190	15.6434 ± 0.1283	0.3644 ± 0.0022	75, 76

[a] Nineteen different decay cases and thirty-four half-life measurements of cluster emission processes have been analyzed in the present work.

[b] $\overline{g}_{\mathsf{se}}$-parameter is associated to each decay case; g_{se}-parameter is associated to the set of the nineteen cluster emission cases.

Table 3 - Quantities involved in calculated half-life values following the present model (ADLM) comparing with experimental data for some selected cluster-decay cases.

Decay case	Knocking frequency [a] $\lambda_0\,[\,10^{29}\,a^{-1}\,]$	Preformation probability [b] S	External barrier penetrability [c] P	Half-life values $[a]$ Calculated [d] $T^{\mathsf{c}}_{1/2}$	Experimental $T^{\mathsf{e}}_{1/2}$	$\Delta\tau = \log(T^{\mathsf{c}}_{1/2}/T^{\mathsf{e}}_{1/2})$
^{230}Th $\rightarrow$ ^{24}Ne	1.073	2.3918×10^{-17}	1.2741×10^{-30}	$(2.12 \pm 0.20)10^{17}$	$(1.34 \pm 0.24)10^{17}$	0.199
^{231}Pa $\rightarrow$ ^{24}Ne	1.093	4.4364×10^{-17}	3.5809×10^{-28}	$(4.00 \pm 0.37)10^{14}$	$(2.44 \pm 0.31)10^{15}$	-0.790
^{232}U $\rightarrow$ ^{24}Ne	1.107	6.0586×10^{-17}	0.8244×10^{-26}	$(1.25 \pm 0.12)10^{13}$	$(0.83 \pm 0.03)10^{13}$	0.178
^{234}U $\rightarrow$ ^{26}Ne	1.058	3.1118×10^{-18}	2.9028×10^{-31}	$(7.25 \pm 0.73)10^{18}$	$(2.92 \pm 0.39)10^{18}$	0.395
^{234}U $\rightarrow$ ^{28}Mg	1.165	1.4710×10^{-19}	0.7862×10^{-28}	$(5.14 \pm 0.56)10^{17}$	$(1.48 \pm 0.21)10^{18}$	-0.459
^{235}U $\rightarrow$ ^{26}Ne	1.042	1.7332×10^{-18}	3.4822×10^{-33}	$(1.10 \pm 0.11)10^{21}$	$(3.59 \pm 1.92)10^{20}$	0.486
^{235}U $\rightarrow$ ^{29}Mg	1.142	3.0083×10^{-20}	4.3567×10^{-31}	$(4.63 \pm 0.51)10^{20}$	$(4.74 \pm 2.79)10^{20}$	-0.010
^{238}Pu $\rightarrow$ ^{30}Mg	1.158	2.7339×10^{-20}	1.6063×10^{-28}	$(1.36 \pm 0.15)10^{18}$	$(3.51 \pm 1.32)10^{18}$	-0.412
^{238}Pu $\rightarrow$ ^{32}Si	1.249	1.5430×10^{-21}	6.8893×10^{-27}	$(5.22 \pm 0.63)10^{17}$	$(6.31 \pm 3.28)10^{17}$	-0.082
^{242}Cm $\rightarrow$ ^{34}Si	1.259	1.0126×10^{-21}	2.6893×10^{-24}	$(2.02 \pm 0.24)10^{15}$	$(4.37 \pm 1.30)10^{15}$	-0.335

[a] $\lambda_0 = 2.192\,a^{-1}(Q/\mu_0)^{1/2}$, [b] $S = \mathrm{e}^{-G_{\mathsf{ov}}}$, [c] $P = \mathrm{e}^{-G_{\mathsf{sp}}}$, [d] $T^{\mathsf{c}}_{1/2} = (\lambda_0 SP)^{-1} \cdot \ln 2$

Table 4 - Data used in obtaining the correlations $\tau_{c,e}$ vs $\mathcal{A}$ (see Fig. 4)*.

Decay case	Q-value (MeV)	u	$c-a$	c	$\mathcal{A}_{\mathrm{T}}$ [MeV·fm]	τ_{c}
^{230}Th $\rightarrow$ ^{24}Ne	57.941552	0.565170	7.8807	11.2365	283.29	17.33
^{231}Pa $\rightarrow$ ^{24}Ne	59.895400	0.577560	7.8801	11.2471	273.94	14.60
^{230}U $\rightarrow$ ^{22}Ne	61.576569	0.583485	7.7641	11.1887	270.07	13.02
^{232}U $\rightarrow$ ^{24}Ne	62.497923	0.595873	7.8817	11.2578	258.88	13.10
^{233}U $\rightarrow$ ^{24}Ne	60.673644	0.579050	7.8825	11.2689	275.58	15.76
^{234}U $\rightarrow$ ^{24}Ne	59.013347	0.563754	7.8832	11.2799	291.42	18.22
^{234}U $\rightarrow$ ^{26}Ne	59.600681	0.571697	7.9977	11.3261	284.39	18.86
^{234}U $\rightarrow$ ^{28}Mg	74.331436	0.611061	8.0950	11.3641	288.50	17.71
^{235}U $\rightarrow$ ^{24}Ne	57.551753	0.550333	7.8840	11.2910	305.84	20.53
^{235}U $\rightarrow$ ^{26}Ne	58.240559	0.559198	7.9985	11.3372	297.54	21.04
^{235}U $\rightarrow$ ^{28}Mg	72.646977	0.597797	8.0958	11.3752	303.29	20.02
^{235}U $\rightarrow$ ^{29}Mg	72.697673	0.599303	8.1483	11.3959	302.26	20.66
^{236}U $\rightarrow$ ^{28}Mg	70.950739	0.584414	8.0967	11.3864	318.72	22.42
^{236}U $\rightarrow$ ^{30}Mg	72.492486	0.599263	8.2010	11.4274	302.85	21.54
^{236}Pu $\rightarrow$ ^{28}Mg	79.898797	0.642010	8.0961	11.3854	261.70	13.28
^{238}Pu $\rightarrow$ ^{28}Mg	76.140347	0.612997	8.0978	11.4075	293.01	18.05
^{238}Pu $\rightarrow$ ^{30}Mg	77.021864	0.622334	8.2023	11.4487	283.96	18.14
^{238}Pu $\rightarrow$ ^{32}Si	91.447368	0.651182	8.2946	11.4842	289.50	17.72
^{242}Cm $\rightarrow$ ^{34}Si	96.814117	0.677292	8.3939	11.5646	267.02	15.31
^{238}U $\rightarrow$ ^{34}Si	85.170917	0.624092	8.3912	11.5221	315.66	23.55
^{238}U $\rightarrow$ ^{30}Mg	69.675316	0.577099	8.2028	11.4497	328.60	25.71
^{232}Th $\rightarrow$ ^{24}Ne	54.845430	0.536032	7.8826	11.2588	314.43	22.34
^{232}Th $\rightarrow$ ^{26}Ne	56.093000	0.550465	7.9965	11.3048	299.92	21.88
^{232}Th $\rightarrow$ ^{28}Mg	68.299530	0.577339	8.0942	11.3428	318.10	23.43

*τ_{e} - values are those listed in Table 2.

Figure Captions

Fig. 1 Shape of the one-dimensional potential barrier for the case of cluster decay $^{238}\mathrm{Pu} \rightarrow {}^{32}\mathrm{Si} + {}^{206}\mathrm{Hg}$. The shaded area emphasizes the overlapping barrier region a–c where the cluster is being formed. The region of the external, separation barrier c–b comprises the Coulomb plus centrifugal (whenever $\ell \neq 0$) contributions to the barrier.

Fig. 2 Reduced, equivalent liquid drop nuclear radius ($r_0 = R/A^{1/3}$) to the average equivalent rms radius of the proton and neutron distributions, R, following the finite-range droplet model—FRDM (2012) by Möller *et al.* [53]. A clear degree of nuclear compressibility is noted when one passes from less-massive nuclei to massive and heavy ones.

Fig. 3 Distribution of the deviation $\Delta\tau = \tau_{\mathsf{c}} - \tau_{\mathsf{e}}$ between calculated, $\tau_{\mathsf{c}} = \log_{10} T^{\mathsf{c}}_{1/2}$, and experimental, $\tau_{\mathsf{e}} = \log_{10} T^{\mathsf{e}}_{1/2}$, half-life-values for the thirty-four measurements of the nineteen different cases of cluster decay analysed in the present work (blue line; see Table 2). For comparison, the red-line distribution has been constructed taking four-hundred-one $\Delta\tau$-values from seventeen studies which contain half-life information on the same exotic cluster decay cases analysed in the present work [22, 23, 29, 70, 77–89].

Fig. 4 Half-life-values, $\tau = \log_{10} T_{1/2}$, plotted against total area of the overlapping plus separation barrier regions, $\mathcal{A}_{\mathsf{T}}$, limited by the potential energy curves and Q-values of the decay processes (see Fig. 1 and Eq. (52)). In part a) are shown calculated data points, τ_{c}, following the present calculation model (see Table 4); the decay cases are identified by different symbols (parent, emitter nuclides in part b), and emitted clusters in part a)); the line is the least-squares linear correlation of $\rho = 0.968$. In part b) are represented the experimental data points, τ_{e} (see Table 2), by using the same symbolism as in part a); the least-squares correlation is in this case $\rho = 0.923$. The distribution of the difference $\Delta\tau = \tau_{\mathsf{fit}} - \tau_{\mathsf{e}}$ is depicted in the inset histogram. Note that three cases of cluster emission from ^{232}Th parent nucleus (■) and two ones from ^{238}U (▼) have been predicted to exhibit $T^{\mathsf{c}}_{1/2} > 10^{22}\,a$, therefore very difficult of being observed.

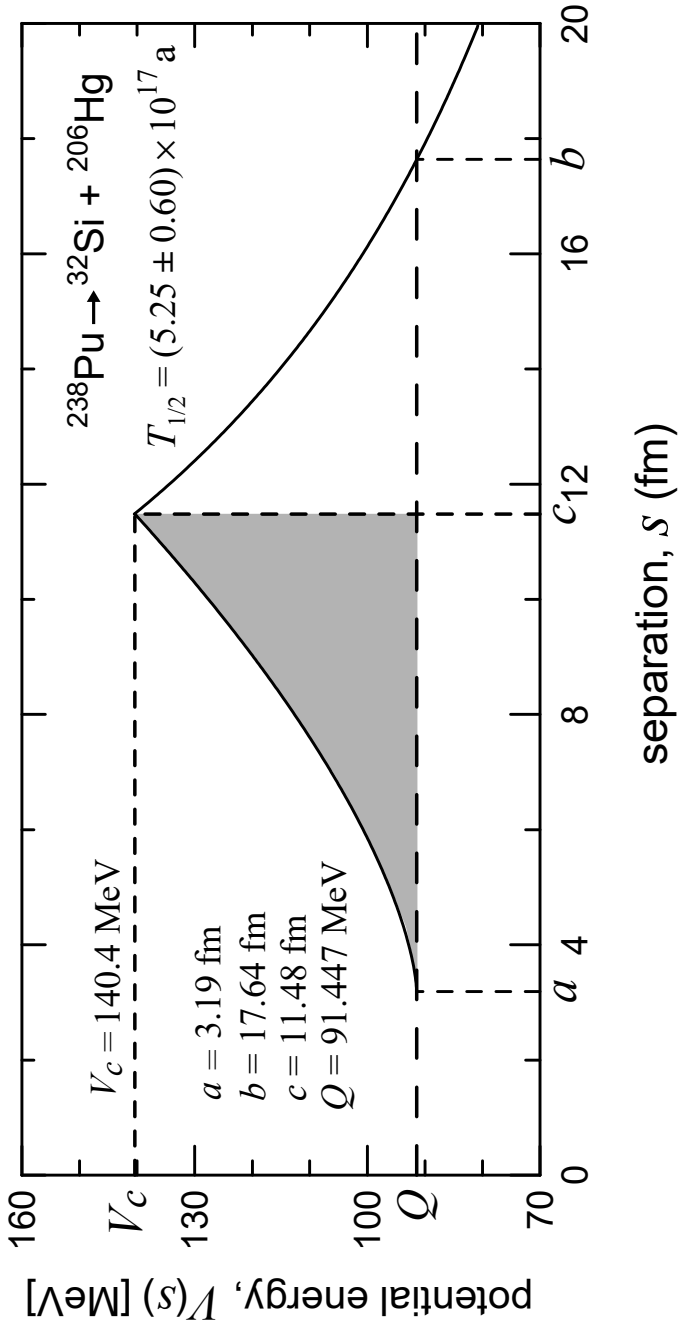
^{238}Pu → ^{32}Si + ^{206}Hg
$T_{1/2} = (5.25 \pm 0.60) \times 10^{17}$ a
$V_c = 140.4$ MeV
$a = 3.19$ fm
$b = 17.64$ fm
$c = 11.48$ fm
$Q = 91.447$ MeV
potential energy, $V(s)$ [MeV]
separation, s (fm)
160
130
100
70
0
4
8
12
16
20
V_c
Q
a
c
b

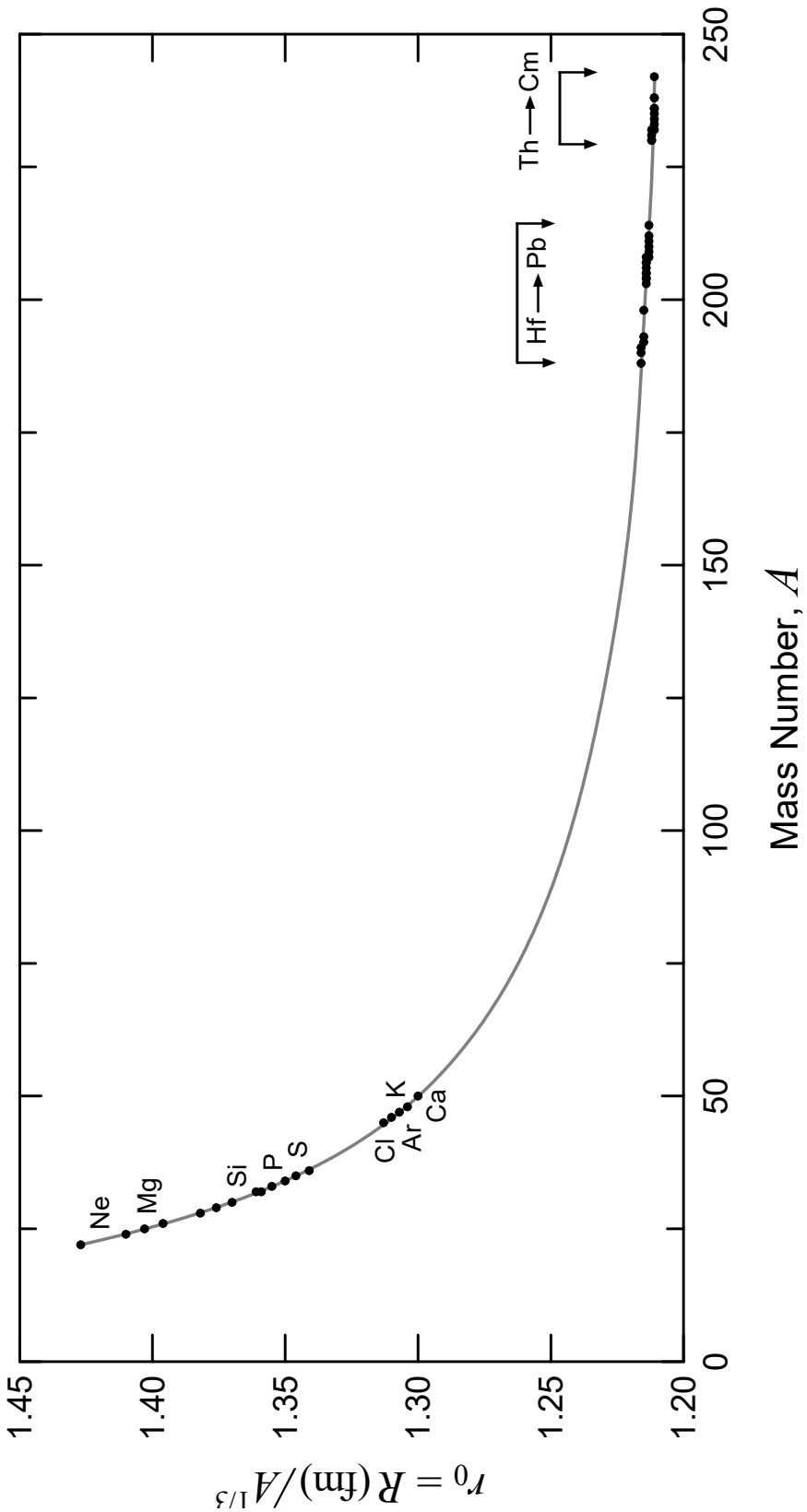
1.45
1.40
1.35
1.30
1.25
1.20
$r_0 = R\,(\mathrm{fm})/A^{1/3}$
0
50
100
150
200
250
Mass Number, A
Ne
Mg
Si
P
S
Cl
Ar
K
Ca
Hf → Pb
Th → Cm

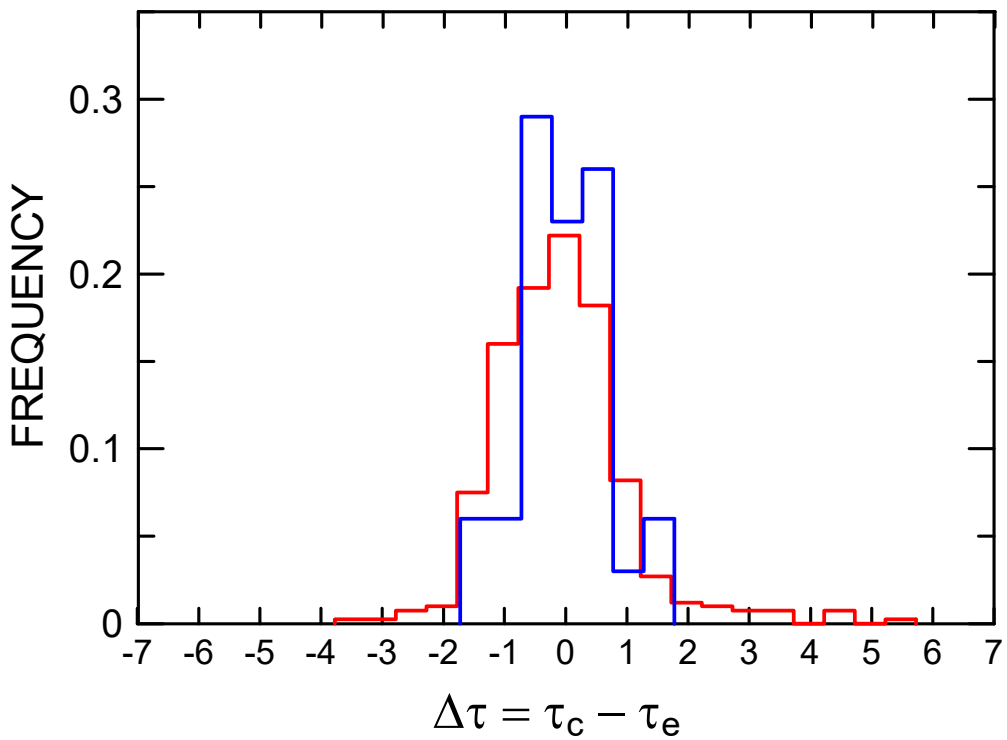
FREQUENCY
0.3
0.2
0.1
0
-7 -6 -5 -4 -3 -2 -1 0 1 2 3 4 5 6 7
$\Delta\tau = \tau_c - \tau_e$

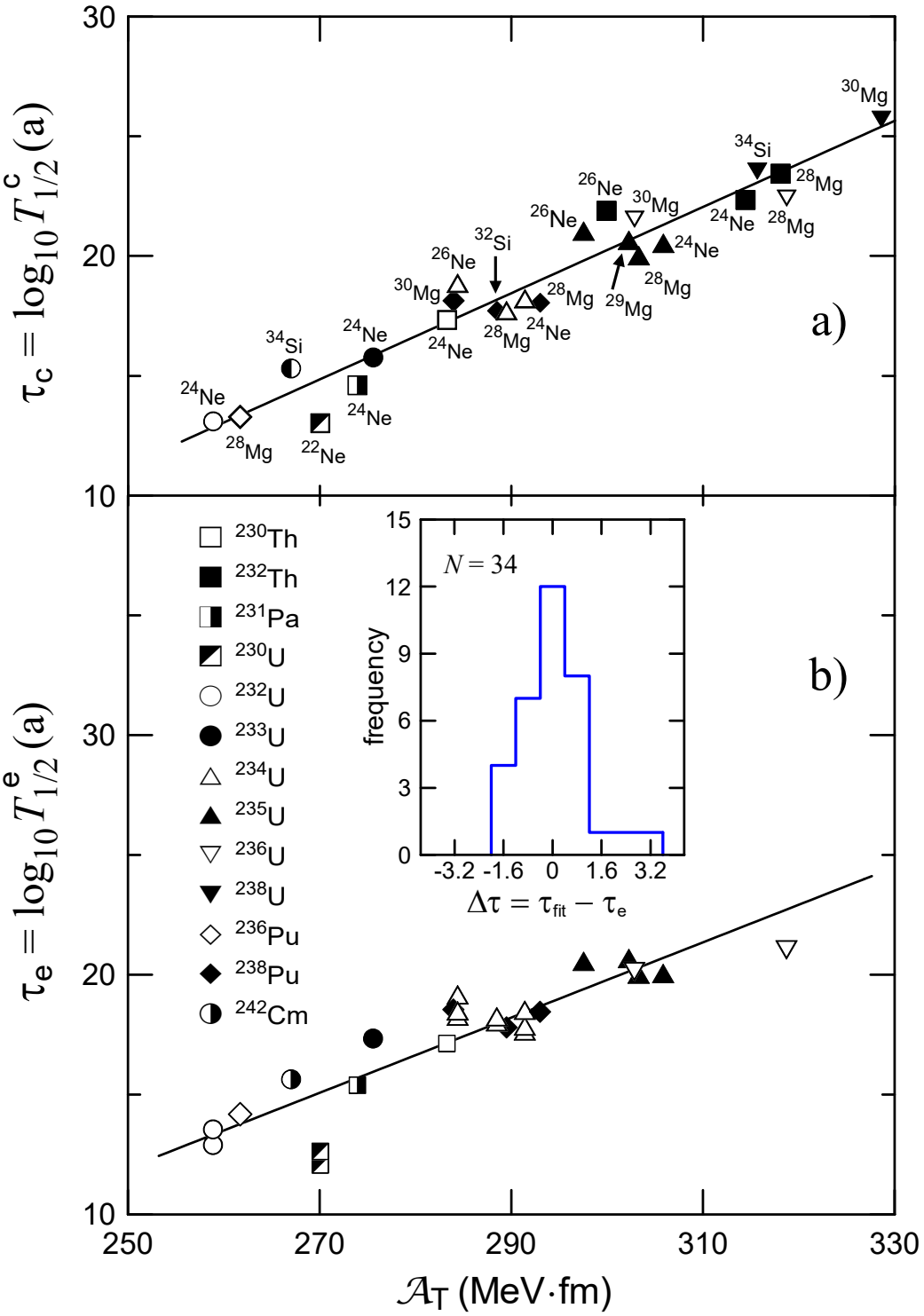
a)
b)
$\tau_c = \log_{10} T^c_{1/2}$ (a)
$\tau_e = \log_{10} T^e_{1/2}$ (a)
$\mathcal{A}_T$ (MeV·fm)
^{230}Th
^{232}Th
^{231}Pa
^{230}U
^{232}U
^{233}U
^{234}U
^{235}U
^{236}U
^{238}U
^{236}Pu
^{238}Pu
^{242}Cm
$N = 34$
frequency
$\Delta\tau = \tau_{fit} - \tau_e$